

TOPICAL ISSUE ARTICLE

Efficiency of laser-induced desorption of D from Be/D layers and surface modifications due to LID

















To cite this article: Mirosław Złobinski *et al* 2020 *Phys. Scr.* **2020** 014075

Recent citations

- [17th international conference on plasma-facing materials and components for fusion applications](#)
Jan Coenen *et al*

View the [article online](#) for updates and enhancements.

Efficiency of laser-induced desorption of D from Be/D layers and surface modifications due to LID

Mirosław Zlobinski¹ , G De Temmerman² , C Porosnicu³ ,
D Matveev¹ , B Unterberg¹ , G Sergienko¹ , S Brezinsek¹ ,
D Nicolai¹ , A Terra¹ , M Rasinski¹ , B Spilker¹ , M Freisinger¹ ,
S Möller¹ , Ch Linsmeier¹ , C P Lungu³  and P Dinca³ 

¹Forschungszentrum Jülich GmbH, Institut für Energie- und Klimaforschung-Plasmaphysik, Partner of the Trilateral Euregio Cluster (TEC), 52425 Jülich, Germany

²ITER Organization, Route de Vinon-sur-Verdon, CS 90 046, 13067 St Paul Lez Durance Cedex, France

³National Institute for Laser, Plasma and Radiation Physics (INFLPR), Atomistilor 409, Magurele, Jud Ilfov, 077125, Bucharest, Romania

E-mail: m.zlobinski@fz-juelich.de

Received 23 September 2019, revised 29 November 2019

Accepted for publication 4 December 2019

Published 24 June 2020



Abstract

For the *in situ* application of LID (Laser-Induced Desorption) as a space-resolved tritium retention diagnostic in ITER, the desorption behaviour of co-deposited deuterium (D) from beryllium (Be) layers is studied. In particular, the desorption efficiency dependence on laser pulse parameters is investigated for pulse durations of 1–20 ms and absorbed energy densities up to 5 MJ m⁻². For these parameter scans homogenous Be/D layers were produced by High Power Impulse Magnetron Sputtering, with 10 μm thickness and 1.6 at% D. Almost 99% of the initial D can be desorbed with a single LID pulse. As the layers show a high D desorption temperature (ca. 800 K) in slow Thermal Desorption Spectrometry, an LID efficiency of only 50% is reached before Be melting. Microscopy reveals that in molten regions holes are formed, which could serve as desorption channels to facilitate gas release above the melting point. Hill formation and cracking are further modifications, but no layer destruction was observed in general.

Keywords: fuel retention, beryllium, tritium monitoring, laser, desorption, FREDIS

(Some figures may appear in colour only in the online journal)

1. Introduction and motivation

Hydrogen isotope retention in fusion devices is problematic due to the losses in the general fuel cycle itself, but mainly due to safety reasons. Because of the latter, the maximum in-vessel tritium (T) inventory is limited in ITER as a safety measure, in case it is completely released to the environment. Experience from the JET ITER-like wall shows that a major contribution to long-term deuterium (D) retention are Be/D co-deposited layers on W divertor components, due to erosion of the Be first wall and co-deposition of fuel in such Be layers of tens of μm thickness [1, 2]. Simulations show that in ITER a comparable formation of Be/D layers can be expected [3]. Therefore, a representative part of the inner divertor baffle of

ITER shall be scanned by a retention diagnostic, named a ‘tritium and deposition monitor’, to obtain a spatially resolved T distribution map [4]. It shall be obtained by *in situ* LID measurements of the fuel retention in laser spots of several mm in size, using a pulsed laser to thermally desorb and quantify the retained gas. Only a few LID experiments on Be and Be layers have been performed in the past [5, 6], however these have been without an extensive laser parameter scan. The main aim of the present work is therefore to determine the LID desorption efficiency for D from such layers in relation to the laser parameters (laser pulse duration, energy, number of pulses). This parametric study has begun on 1 μm-thin Be/D layers with high D fraction [7]. Here, we perform a similar parameter scan for 10 μm-thick layers and

significantly lower D content to extend the knowledge of the desorption behaviour for different layer characteristics that might be more relevant to ITER. Due to improved homogeneity of these new layers we can even extend the laser parameter variations. Additionally, an improved layer production method enables us to completely exclude uncertainties originating from delamination which occurred in the previous study [7].

2. Sample production

Homogeneous D-containing layers are a prerequisite for such a parametric study. As the samples should simulate the expected Be layers in the ITER divertor, ITER grade tungsten W-‘IGP’ by Plansee with grains elongated perpendicular to the surface was selected as a substrate. Large samples with a size of $35 \times 35 \times 5 \text{ mm}^3$ (for up to 49 laser spots) and $5 \times 5 \times 5 \text{ mm}^3$ for Thermal Desorption Spectrometry (TDS) were used. The substrate roughness was 100–150 nm. The Be layers were created in INFLPR in Bucharest, where the substrate was cleaned for 5 min with methyl alcohol at 35 °C, for 5 min with caustic soda at 55 °C, for 10 min with distilled water at RT (room temperature) and finally rinsed with distilled water. In the plasma chamber the substrate was cleaned for 30 min by a DC glow discharge (300 V, 250 mA) before the Be layer was deposited by means of two DC and two High Power Impulse Magnetron Sputtering (HiPIMS) magnetrons in an Ar:D gas mixture of 20:1 at a total pressure of ca. 2 Pa, similar to the process in [8]. The layer thickness of 10 μm was verified on Si witness samples exposed simultaneously with the large and four small samples in the same coating run on SEM images of cross sections.

3. Homogeneity analysis

To verify the homogeneity of the layer, NRA (Nuclear Reaction Analysis) and LID [9, 10] were performed in a similar way as for the case of a 1 μm -thin layer described in [7] in the FREDIS device [11] and the NRA chamber in Jülich. The same laser setup was used (3 mm laser spot diameter, ca. 1 mm NRA beam size, etc). The only difference was that the NRA beam energy was reduced to 4.15 MeV to improve the separation of the Be and D peaks. The good stability of the layer implies that no compensation for delaminated layer fragments was needed for the interpretation of the NRA data. In LID an improvement was made as the laser energy could now be measured directly in front of the vacuum window by a new joulemeter (Gentec-eo UP19K-15S-W5-INT-D0), which is capable of measuring all laser energies for all pulse durations of the laser, hence reducing the uncertainty in laser energy.

The homogeneity analysis was performed by NRA and LID independently. The NRA measurement points, which are located on the unheated layer between the laser spots, are marked by yellow squares in figure 1(a). The LID homogeneity analysis used 5 ms pulses with 27 J absorbed energy (black circles) resulting in temperatures of 1700–2200 K, i.e. above the Be melting temperature. The NRA results for

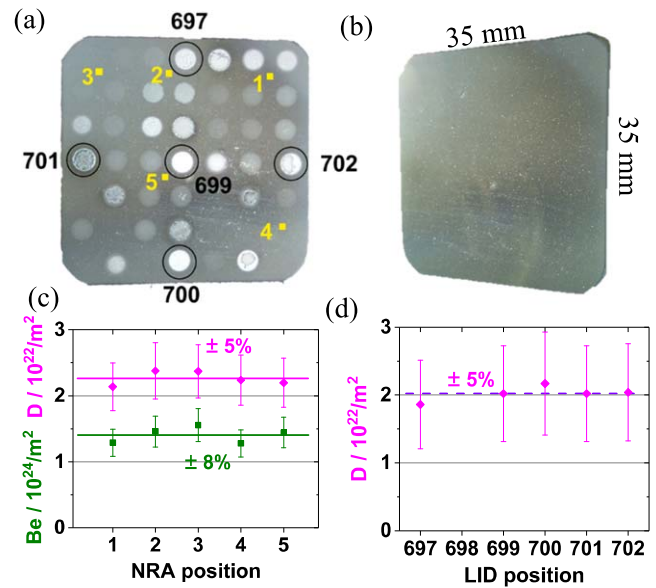


Figure 1. Homogeneity analysis of W sample with 10 μm Be layer containing 1.6 at% D: (a) measurement positions; (b) sample before analysis; (c) NRA analysis; (d) LID-QMS analysis.

the D and Be concentration show a very small variation of $\sigma = \pm 8\%$ (standard deviation) for Be and only $\pm 5\%$ for D. The desorbed amount is very similar to the NRA value. The variation of the D signal measured by LID in combination with Quadrupole Mass Spectrometry (QMS) is as small as in NRA. Thus, both methods prove the excellent layer homogeneity despite an inhomogeneous optical appearance of the sample surface showing differently coloured regions (figure 1(b)). The ratio of the NRA data results in D concentrations of 1.5–1.7 at% and on average 1.6 at% D with an absolute value of $2.3 \times 10^{22} \text{ D m}^{-2}$.

4. LID efficiency

The laser pulse duration was varied within 1 and 20 ms and the absorbed laser energy density was in the range of 0.4 and 4.8 MJ m^{-2} . The latter was estimated according to the measured total reflectivity of 21% (at 1064 nm wavelength) on this sample and the laser energy which was measured with the calibrated joulemeter in front of the AR coated vacuum window. Due to the AR coating which leads to a reflection below 1%, the uncertainty in applied energy is very low, however the uncertainty due to the change of reflectivity as a result of the increasing temperature remains, and is estimated to account for a possible error of 15%.

Some positions were heated repeatedly by several laser pulses, but we first discuss the results of the 1st shot on each position in figure 2. The thick lines are only guides for the eye for the five pulse durations used, however they indicate a twofold desorption behaviour that is particularly pronounced for the 2.5 and 5 ms pulses. The slope of the desorption increase is smaller for the higher laser energy densities.

This is attributed to the onset of melting, as will be discussed for figure 2(b). These two pulse durations reach

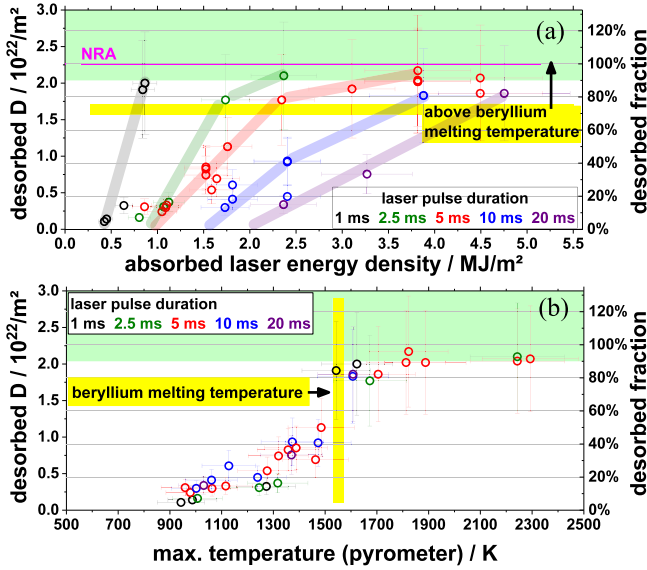


Figure 2. Dependence of the LID-QMS efficiency on: (a) absorbed energy density; (b) maximal temperature measured by the pyrometer.

desorption values very close to the average NRA value for the unheated layer (see above). For the 20 ms pulses the maximal available laser energy was used. The highest data point for the 10 ms pulse does not reach the high desorption of the shorter pulses, either, although similar absorbed energy densities were reached as for the 5 ms pulses. This is probably also just due to a data scatter which seems to be in that range, e.g. comparing the 5 ms pulses with 4 and 4.5 MJ m⁻². Thus, the highest values for the two long pulse durations are probably just at the lower range of the scatter. As the surface area was additionally limited due to a higher spot separation for the 20 ms pulses (7 mm centre-to-centre distance due to lateral heat diffusion instead of 5 mm for all others) the statistics are low for the long pulse durations. Thus, for the 10 and 20 ms pulses only a maximum of ca. 80% desorption relative to the NRA value is reached. The right axis shows this desorption efficiency which is the ratio of the LID value to the average of the NRA values of the unheated layer (cf. the pink line in figure 1(c)). The efficiency is slightly higher if it is instead related to the LID maximum, as the highest LID value is slightly below the NRA average. However, as seen further in figure 4, the measurement of the remaining D in the 20 ms laser spot with highest laser energy measured by NRA will show a desorption of more than 98% for the spot centre (inner 1 mm diameter). Thus, the smaller LID-QMS value shown here is due to the uncertainty in the QMS measurement, or the lower temperature gradient at the spot edge, due to the long duration and hence the smaller hot central part. All shorter pulse durations reach a desorption fraction of 90% and above. The maximum desorption fraction is similar for the different pulse durations investigated. In conclusion, a very high desorption efficiency above 90% can be achieved for pulse durations in the tested 1–20 ms range for this kind of layer.

Figure 2(b) shows the same LID-QMS data, but against the maximal temperature measured in the laser spot centre by the spot pyrometer using the one-colour mode (at 1.66 μ m)

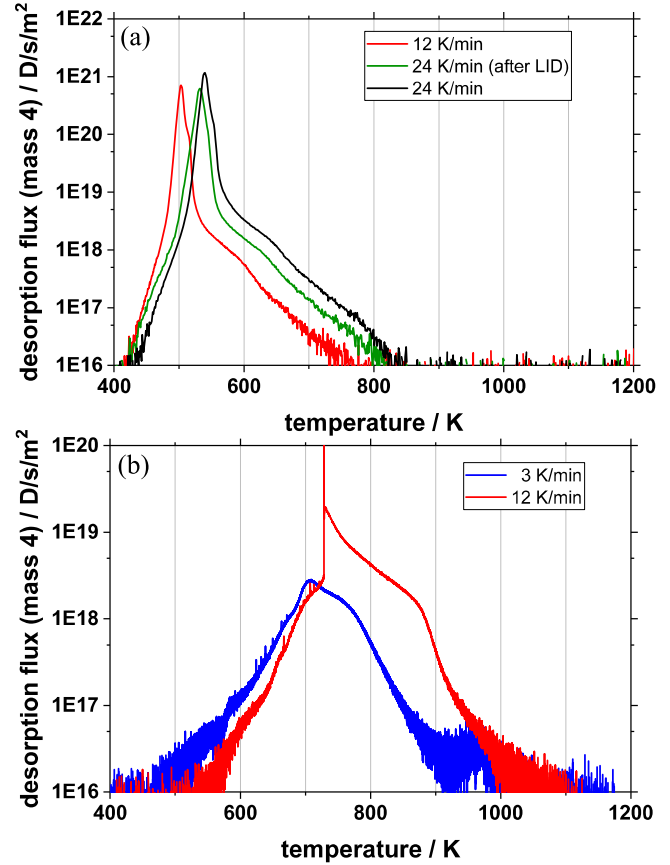


Figure 3. TDS spectra of: (a) 1 μ m Be/D layer with 30 at% D and (b) 10 μ m thickness with 1.6 at% D with a 300 K higher desorption temperature.

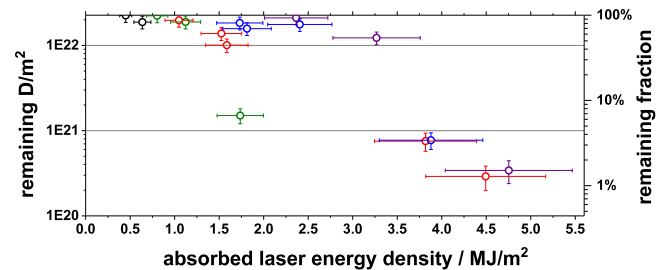


Figure 4. NRA measurement of remaining D inside the laser spot centre (ca. 1 mm NRA beam size), 4.15 MeV ³He⁺⁺ with incidence angle 0, scattering angle 150°, exit angle 30°; evaluated with SIMNRA [12].

and the emissivity measured at this wavelength ($\epsilon_1 = 0.68$). The data show a general desorption increase with higher temperature, as expected. In contrast to the layer with high D content (cf. [7]) only a maximal desorption fraction of 50% could be reached before the onset of melting. At the Be melting temperature a jump to 80% (with two exceptions) is observed and a further slower increase towards complete desorption. This jump corresponds to the slope change observed in the previous energy representation, showing that at the melting onset a considerable fraction of D is desorbed. The reason for this will be discussed in the surface morphology section below. The two exceptions (for the 2.5 and

10 ms data points) are presumably owing to an incorrect temperature measurement due to damage of the layer surface in these spots that occurred during the laser pulse. Thus, the temperatures would be probably below the melting temperature if the layer had the same adhesion as in the other spot positions.

Above the melting point still a further desorption increase can be seen, which is probably due to the fact that the whole laser spot surface melts does not melt at once, as will also be shown in the morphology section. Initially, only some elevated structures (which we will call elevations) are molten, and not the regions in between. With increasing laser energy consecutively larger regions are molten. The hypothesis is that only then can they release the D fraction that is not desorbed below the melting temperature.

The maximum of LID efficiency can be cross-checked by NRA measurements inside the laser spots in direct comparison to unheated layer regions outside the laser spot. Not all laser spots could be measured, as some damaged spots had to be covered by carbon tape to prevent flaking of Be in the NRA chamber.

The retention minimum was found between 1 and 2% of the initial D content with error bars including 1% of remaining D. Therefore, we can state that for this kind of layer, the LID efficiency can reach very high values of ca. 99%, however only by melting.

Comparing the LID results with the laser flash heating of PISCES layers [6] shows relatively good agreement, particularly for the magnetron coated layers. They desorbed ca. 25% of D by 10 ms pulse duration at 2 MJ m^{-2} absorbed laser energy density. In our case this efficiency is already reached for slightly lower energy densities but this is within the error bars, and the blue guideline in our results (figure 2(a)) shows that these values are slightly above the trend. Hence, the guideline itself runs quite exactly through their data points. However, at the low energy end, the agreement is not that good. Their 10% efficiency is reached around 0.3 MJ m^{-2} , while it is above 1.5 MJ m^{-2} in our case for 10 ms. Rather, their desorption threshold fits to our 1 ms pulse duration. In terms of temperature the agreement is the other way around: the desorption threshold is similar, with 850 K for their case and 900–1000 K for our case. Here, the high temperature end shows a larger disagreement, where their highest efficiency of 25% is reached around 1000 K, while we see only half of this efficiency at this temperature. In general, the agreement is good, but obviously there is a different correlation of temperature to absorbed laser energy for the two data sets. The agreement of this layer is much better than for the high D concentration layer of $1 \mu\text{m}$ thickness (cf. [7]). This can be also seen comparing the TDS spectra of our $10 \mu\text{m}$ layer and the TDS of the layers in [6]. Their TDS spectrum is dominated by the high temperature peak around 800 K, which is also the case for our layer at comparable heating rates (18 to 12 K min^{-1} , cf. figure 3(b)). The low temperature peak, which their magnetron layers show as a minor contribution around 500 K, does not appear in our low-D layer, but is the dominant peak for our high-D layer

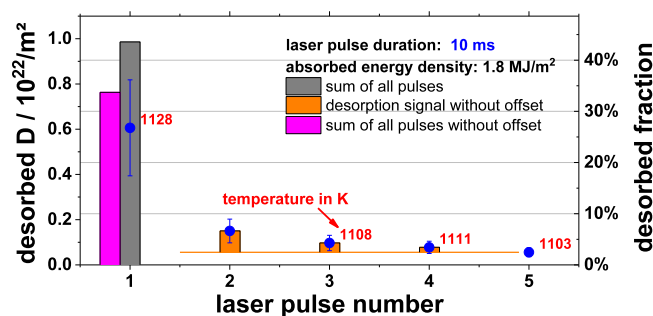


Figure 5. Multiple laser pulses on the same spot.

(figure 3(a)) at very similar peak position for the slower heating rate of 12 K min^{-1} .

Hence, the TDS peak position seems to be the main parameter that determines the LID efficiency behaviour. The shift of the TDS peak by 300 K between our high-D and low-D case leads to a factor of two decrease in LID efficiency below the melting point, since in the high-D case complete desorption is reached before significant melting. There, only few edges and corners of some delaminating layer fragments were molten, however the majority of the layer showed sharp edge structure and thus no melting.

The general conclusion we draw is that the LID efficiency before the melting point is determined by the desorption peak temperature and thus the binding energy of D as shown by the TDS spectra. The activation energy for D diffusion has been determined from the temperature shift of the TDS spectra of the small samples for different heating rates according to the Polanyi–Wigner theory. For the low temperature desorption a value of 0.4–0.5 eV was determined and for the high temperature desorption 1.1 eV. The LID efficiency reduces the higher these values increase. However, including the melting regime, LID can reach nearly complete desorption in both kind of layers. This is important for the application of LID as T diagnostic as complete desorption—or a lower but constant desorption efficiency—is a prerequisite.

If laser induced melting of the layer is not tolerated in ITER, then multiple heating of the same spot has been suggested as a possibility to desorb the layer completely with multiple laser pulses. This has been demonstrated in 1D simulations [4]. However, our experimental attempts to increase LID efficiency in such a way often ceased after few laser pulses as the desorbed amount of the subsequent pulses decreased very fast and a constant desorption signal was reached after few pulses (cf. figure 5). This constant value is interpreted as unavoidable desorption from the laser edge due to two effects. At the laser edge a strong spatial gradient in D concentration is present, thus D diffusion can occur even if the temperature distribution is always the same for each pulse. As this constant ‘desorption offset’ is only few percent of the D content in the layer, there is a huge D reservoir outside the laser spot and thus this offset signal does not decay strongly. A second effect might also play a role, namely surface modifications such as change of reflectivity, cracking or hill formation. It can be observed that some of these slowly

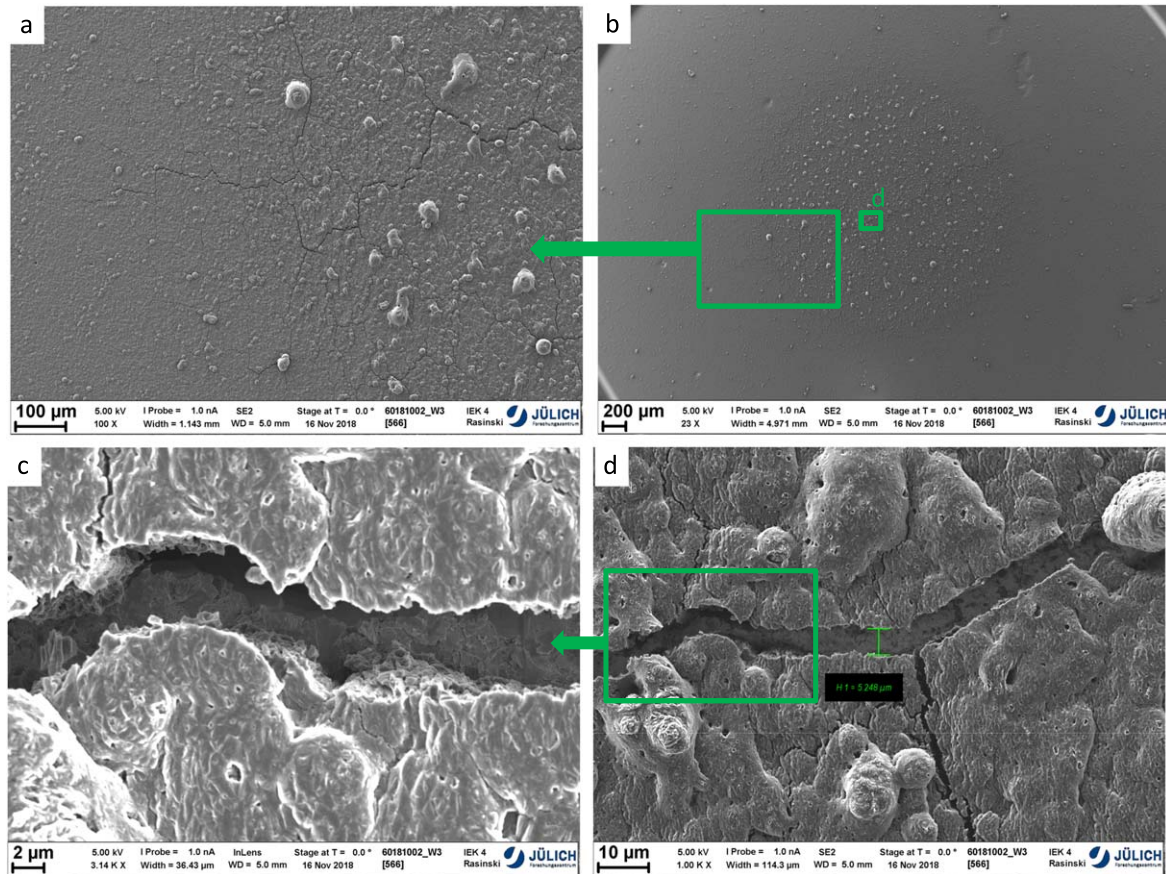


Figure 6. SEM images of a 10 μm Be layer with 1.3 at% D (averaged) and very good adhesion to the W substrate after 1 strong LID pulse ($E_{\text{abs}} = 26.5$ J absorbed energy, $t_p = 10$ ms, $T_{\text{pyro}} = 1529$ K): (a) zoom of laser spot edge; (b) whole laser spot 3 mm diameter; (c) zoom of (d) shows possible crack in the substrate; (d) a broad crack with crack width of 5 μm .

evolve from pulse to pulse. These small changes of the surface properties can affect the reflectivity and thus absorption properties of the layer which may lead to increased temperatures in very localised small regions of the laser spot and thus desorb additional D from these regions. For judging the effect of subsequent laser pulses this ‘desorption offset’ (the orange line in figure 5) has to be subtracted from the signal of the subsequent pulses. In this representative example shown here, the desorption can apparently be increased by more than ten percentage points when summing the pulses including this offset (the grey bar). But after subtraction of the desorption offset from the subsequent pulses, the LID efficiency is only increased by few percentage points.

5. Surface morphology

SEM images of the LID spots show surface morphology changes due to the laser heating. For layers with very good adhesion to the substrate like the sample discussed here, no delamination is observed in the SEM surface analysis except for some very rare and small fragments. The main surface modifications are cracking, melting and elevations of the layer.

5.1. Cracking

The crack length is often similar or even larger than the laser spot size, such as in figure 6(b) from the upper right to lower left corner. The cracks reach quite far into the spot edge (figure 6(a)). The largest crack width that could be observed was ca. 5 μm (cf. figures 6(d) and (c)). In the analysed cracks, a bottom could usually always be seen, not particularly deep below the top surface (such as in figure 6(d) on the right hand side). It is not clear whether this bottom ground is the W substrate or a deeper part of the Be layer. The brightness of the bottom also does not provide a definite answer, as the brightness is reduced due to the shadowing effect of the narrow crack walls. Due to the visible crack bottom, it is more likely that the W substrate is typically not cracked in most instances. Only in one case could a deeper crack depth be observed (figure 6(c)), which might also reach into the substrate. However, the presence of W cracks that are parallel to the layer cracks but hidden by the crack walls cannot be ruled out.

Below melting onset the laser spot is hardly visible (e.g. Figure 8) as cracking is the only obvious surface modification. Fairly dense crack networks were often observed with mostly thin cracks and crack distances in the order of ca. 50 μm (cf. figure 9).

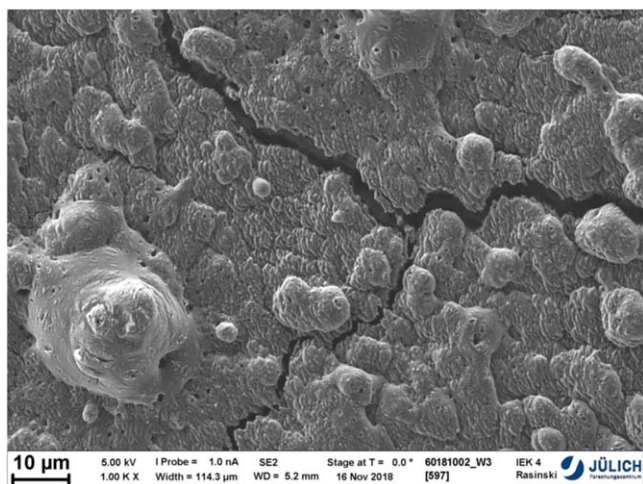


Figure 7. Molten and unmolten regions in one laser spot at the Be melting point (10.7 J absorbed, 2.5 ms, 1533 K); SEM image of the same sample as above.

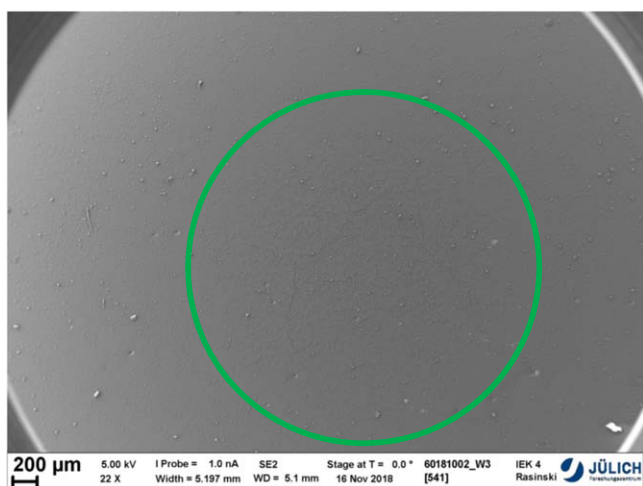


Figure 8. For good adhesive layers cracking is the only surface modification below the melting point (12.2 J absorbed, 5 ms, 1313 K); SEM image of the same sample as above.

5.2. Melting

Melting is obvious, particularly on the layers with low D content, as the original microstructure of the material has very sharp edges, in contrast to the high D content case. These edges are smoothed by the melting process, while different degrees of smoothing can be observed with increasing laser intensity (cf. figure 10). The micro-cracks in the material often seem to appear along the grain boundaries (cf. figure 10(b)). However, it should be noted that several places were found where the crack also appears across the grain, separating it into two parts. The smoothing effect of the melting process is even more pronounced on the elevations that are formed within the laser spot. At the melting threshold these elevations and hills seem to melt first, or at least show stronger surface smoothing than the flat surface between them (cf. figure 7). On the latter areas the sharp microstructure can

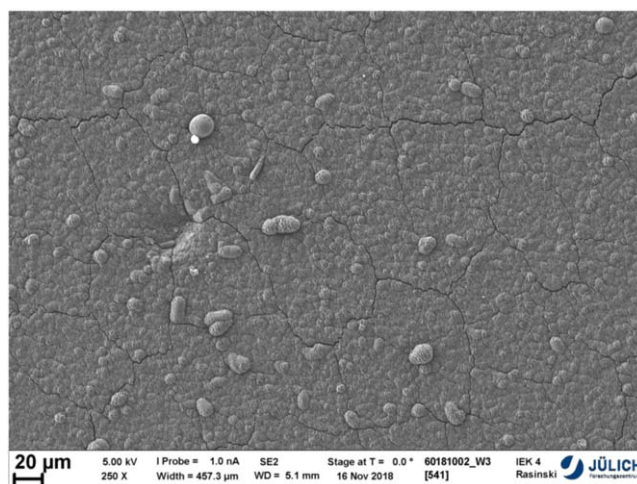


Figure 9. Crack network inside a laser spot with 12.2 J absorbed, 5 ms, 1313 K; SEM image of the same sample as above.

still be seen, while the hills and elevations have a much smoother appearance. The melting process does not lead to significant Be evaporation, as the measured Be amount seen by NRA in the laser spots is in the range of 0.92–1.1 of the average Be value of the unheated areas, with a standard deviation below 6%. This also confirms that no layer material is lost due to other release processes such as delamination.

5.3. Surface elevations

On the molten areas, which first appear at the hills and elevations, and with higher temperature extend to the full laser spot, many sub-micrometer holes can be observed on the surface (cf. figures 6(c) and (d)). In some cases the size of the holes increases to several micrometers. Our hypothesis is that these holes represent openings through which the desorbing gases are released. Then, the formation of the elevations could be a result of the desorption process and the expanding gas itself. These openings could thus serve as desorption channels or pores that are opening only on molten regions of the laser spot. Their appearance and the increase of the molten area could be the reason for the strong step in desorption at the melting temperature discussed in relation to figure 2(b). Another interpretation is similar to the interpretation of the Be hills in [7], where the cracked Be hills are considered to possibly have formed as a result of the larger expansion of Be, compared to W building hills at mechanically weak points where the contact to the substrate is lower. Although the appearance and characteristics of those cracked Be hills and the molten Be elevations here are very different, the reason for their formation could be similar.

Only in a very few spots and only for intense pulses above Be melting temperatures could microscopic delamination be observed on the present sample, which shows good adhesion in general. Even in these rare cases only very few (ca. 5) fragments are missing, in one laser spot of less than 60 μm in size.

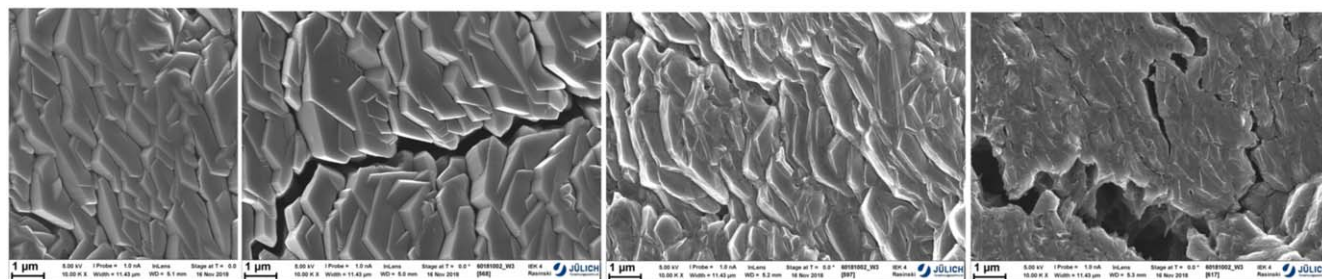


Figure 10. Microstructure evolution with increasing laser heating: (a) original, unheated layer; (b) 10 ms, 1013 K; (c) 2.5 ms, 1533 K; (d) 20 ms, 1519 K. SEM images of the same sample as above.

6. Summary and conclusion

For Be/D layers of 10 μm thickness with 1.6 at% D on ITER grade W, nearly complete D desorption could be achieved with LID pulses of 1–20 ms duration, as shown by NRA in the spot centre. The highest desorption detected by LID-QMS is achieved for pulse durations of 2.5 and 5 ms. Until the onset of melting a desorption efficiency of ca. 50% was found which is a factor of two lower compared to previously studied layers of 1 μm thickness with 30 at% D [7]. This is probably due to the 300 K higher desorption temperature seen in the TDS spectra of these layers. Due to an improved sample preparation process the layers in the present study are highly homogenous and have good adhesion to the substrate. Thus, the only surface modification due to laser heating is cracking, for temperatures below the melting point. With the onset of melting the formation of hills or elevations is observed, which melt first, before larger areas of the laser spot. Molten regions show holes or pores that are interpreted as gas desorption channels, which fits with the observation that the desorption efficiency jumps at the melting point, as the gases might be released more easily via these channels.

If these thicker layers represent a good approximation to the co-deposited layers in ITER, then LID can be applied as T diagnostic, since almost complete D desorption can be achieved. However, this only holds if melting of the surface can be tolerated in ITER. A beneficial advantage of LID is that only gases are released but no Be is released, even during melting. Thus, no strong influence of the main plasma is expected. As a next step, LID studies of Be layers deposited in fusion devices are needed to assess whether the magnetron sputtered layers are reactor relevant, i.e. whether they behave similarly during LID.

Acknowledgments

This work has been carried out within the framework of the EUROfusion Consortium and has received funding from the Euratom research and training programme 2014–2018 and 2019–2020 under grant agreement No 633053. The views and

opinions expressed herein do not necessarily reflect those of the European Commission or of the ITER organization.

Work performed under EUROfusion WP PFC [13].

ORCID iDs

Mirosław Zlobinski <https://orcid.org/0000-0002-1395-7165>

G De Temmerman <https://orcid.org/0000-0002-4173-0961>

C Porosnicu <https://orcid.org/0000-0003-0561-0644>

D Matveev <https://orcid.org/0000-0001-6129-8427>

B Unterberg <https://orcid.org/0000-0003-0866-957X>

G Sergienko <https://orcid.org/0000-0002-1539-4909>

S Brezinsek <https://orcid.org/0000-0002-7213-3326>

D Nicolai <https://orcid.org/0000-0003-1260-8796>

A Terra <https://orcid.org/0000-0003-0638-6103>

M Rasinski <https://orcid.org/0000-0001-6277-4421>

B Spilker <https://orcid.org/0000-0001-9921-0291>

M Freisinger <https://orcid.org/0000-0001-7052-668X>

S Möller <https://orcid.org/0000-0002-7948-4305>

Ch Linsmeier <https://orcid.org/0000-0003-0404-7191>

C P Lungu <https://orcid.org/0000-0003-2955-0009>

P Dinca <https://orcid.org/0000-0003-4383-9941>

References

- [1] Brezinsek S et al 2015 *Nucl. Fusion* **55** 063021
- [2] Heinola K et al 2015 *J. Nucl. Mater.* **463** 961–5
- [3] Schmid K et al 2015 *Nucl. Fusion* **55** 053015
- [4] Temmerman G D et al 2017 *Nucl. Mater. En.* **267–272** 12
- [5] Keroack D and Terreault B 1994 *J. Nucl. Mater.* **212–215** 1443–7
- [6] Yu J H et al 2013 *J. Nucl. Mater.* **1150–1154** 438
- [7] Zlobinski M et al 2019 *Nucl. Mater. En.* **19** 503–9
- [8] Dinca P et al 2017 *Surface & Coatings Tech.* **321** 397–402
- [9] Zlobinski M et al 2013 *J. Nucl. Mater.* **1155–1159** 438
- [10] Zlobinski M et al 2011 *Fus. Eng. Des.* **86** 1332–5
- [11] Zlobinski M et al 2019 *Fus. Eng. Des.* **146** 1176–80
- [12] Mayer M 1997 *SIMNRA User's Guide, Report IPP 9/113, Max-Planck-Institut für Plasmaphysik* (Germany: Garching)
- [13] Brezinsek S et al 2017 *Nucl. Fusion* **57** 116041